

# Sulfurization temperature dependent properties of tin mono-sulfide thin films

M. Gurubhaskar, Narayana Thota, A.C. Kasi Reddy, Y.P. Venkata Subbaiah\*

Department of Physics, Advanced Materials Research Laboratory, Yogi Vemana University, Kadapa, Andhra Pradesh 516003, India

\*Corresponding author: Tel: (+91)9966248876; E-mail: subbaiah@gmail.com

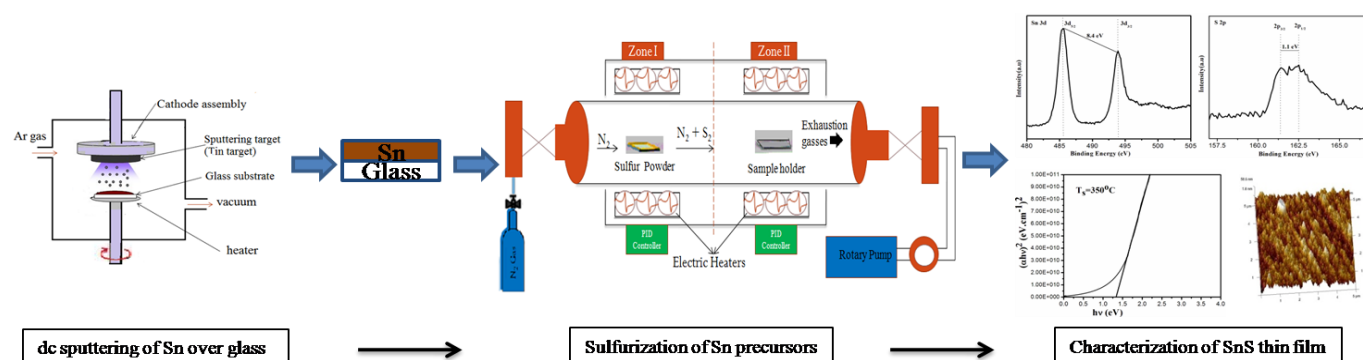
Received: 31 March 2016, Revised: 30 September 2016 and Accepted: 01 November 2016

DOI: 10.5185/amp.2017/806

www.vbripress.com/amp

## Abstract

Tin mono-sulfide thin films were prepared using a two-step process consisting of DC sputtered deposition of Sn precursors over glass substrate held at 150 °C, followed by sulfurization for 1 hour at different temperatures ranging from 250 °C to 400 °C. The influence of the sulfurization temperature on resultant films was studied in terms of its structure, morphology and opto-electronic properties. X-ray diffraction study revealed that the films sulfurized at lower temperature (~250 °C) had prominent SnS<sub>2</sub> phase in addition to SnS. A single-phase tin mono-sulfide planes corresponding to orthorhombic structure has been observed at 300 °C and found to be highly crystalline at 350 °C. Further, three distinct Raman modes observed at 95, 190 and 218 cm<sup>-1</sup> for Sn precursors sulfurized at 350 °C, strongly supporting the formation of single phase SnS. The optimized SnS film showed a direct band gap of 1.35 eV with an absorption coefficient of 5 x 10<sup>4</sup> cm<sup>-1</sup>. The valence states of Sn (+2) and S (-2) determined from X-ray photoelectron spectroscopy analysis for Sn precursors sulfurized at 350 °C, indicating the existence of SnS. These films had stoichiometric atomic ratio of Sn/S ~ 1 with surface roughness of 20 nm. All the films have shown p-type conductivity and the Sn precursors sulfurized at 350 °C exhibited relatively high conductivity of 0.947 x 10<sup>-2</sup> (Ω cm)<sup>-1</sup>. The optoelectronic properties of SnS films reported in the present work would be highly suitable for device fabrication and promising as an alternative absorber for thin film solar cells. Copyright © 2017 VBRI Press.



**Keywords:** SnS films; sputtering and sulfurization; Raman scattering; optical transmittance; X-ray photoelectron spectroscopy.

## Introduction

In recent years, alternative to CuInGaSe<sub>2</sub> (CIGS), the quaternary and ternary compounds like Cu<sub>2</sub>ZnSnS<sub>4</sub> (CZTS) and Cu<sub>2</sub>SnS<sub>3</sub> etc., are emerging as promising photovoltaic materials for the fabrication of low-cost and environmentally benign solar cells [1-3]. However, the issues related to the single-phase growth of CZTS such as co-existence of secondary phases and narrow phase region in phase diagram of CZTS, strongly demonstrating research towards novel and simpler materials [4, 5].

Moreover, the existences of secondary phases are detrimental to obtain higher efficiencies. Several new materials have been proposed alternative to CZTS in recent past [6]. Amongst, SnS is a simple binary absorber material [7], which has optimum energy band gap of 1.3 eV and high absorption coefficient of 10<sup>5</sup> cm<sup>-1</sup> with p-type electrical conductivity and hence most attractive for absorber material in thin film photovoltaic applications [8, 9, 10]. SnS belongs to IV-VI group of semiconductor compounds, where tin and sulfur acts as cation and anion respectively. SnS is a layered semiconductor with a weak

van der Waals bonding between the different layers and crystallizes in orthorhombic structure [10]. A variety of deposition techniques such as electro-deposition [11, 12], evaporation [13-15], chemical vapor deposition [16], atomic layer deposition [17, 18], plasma-enhanced CVD [19], spray pyrolysis [20, 21] and brush plated technique [22] has been successfully demonstrated for the growth of SnS thin films. Although there have been several investigations, to date, SnS has demonstrated conversion efficiency of 3.8 % using thermal evaporation [23], which is far behind from its predicted theoretical efficiency of 24 % and also from earlier counterparts [24, 25, 26]. The low conversion efficiencies of SnS strongly demanding further systematic and in-depth research on this material [27, 28]. Hence, in the present study, an attempt has been made to synthesize device quality SnS using a two-step methodology of sputtering followed by sulfurization. The present paper reports the successful synthesis of SnS films and the effect of sulfurization temperature on the physical properties of SnS films.

## Experimental

### Materials and methods

SnS films were prepared by using two-step process of sulfurization of sputtered Sn precursors. In the first step, the Sn precursor was deposited on soda lime glass ( $7.5 \times 2.5 \text{ cm}^2$ ) substrate at temperature ( $T_s$ ),  $150^\circ\text{C}$  using DC Magnetron sputtering unit (Model -VRT SPU 06D, Bengaluru). Prior to Sn deposition, the substrates were ultrasonically cleaned with double de-ionized water followed by acetone wipe off. The 4N pure (99.99 %) Sn sputter target with 2" dia and 3 mm thickness purchased from Testbourn Ltd., UK has been used in the present study. The target was made to function in sputter down configuration with magnetron assembly embedded in it by facing normal to the substrate. The distance between source and substrate was set to 5 cm by adjusting the target assembly/substrate holder vertically. Prior to deposition, the base chamber was evacuated to  $\sim 5 \times 10^{-5}$  mbar and Ar pressure was set to 0.20 mbar using mass flow controller. The Sputter power for Sn was optimized as 40 W for better glow discharge and sputtering yield. The substrate rotation was fixed at 6 rotations per minute in order to ensure uniform deposition. In the second step, the sputtered Sn precursor films were sulfurized using two zone tubular furnace of 1.2 m length with 50 mm inner diameter and 55 mm outer diameter (INDFURR, Chennai). The  $\text{N}_2$  gas cylinder and rotary pump was connected to the two ends of the quartz tube for vapor carrier and evacuation, respectively. The Molybdenum boat containing elemental sulfur powder (Aldrich-414980, Germany) was placed in Zone-I and sputtered Sn precursors (1cm x 1 cm) kept in graphite holder was placed in Zone-II. The temperature of sulfur powder zone was maintained constantly at  $130^\circ\text{C}$  and the temperature of Sn precursor zone was varied from 250 to  $400^\circ\text{C}$  in multiples of  $50^\circ\text{C}$  and set at each temperature for 1 hour. After the sulfurization, the samples are allowed for natural cooling to room temperature. Throughout the

annealing process the pressure was maintained around 20 mbar in quartz tube.

### Characterization

The structural properties of Sn precursors sulfurized at different temperatures was studied using X-ray diffractometer (Rigaku Miniflex 600, Japan) with  $\text{CuK}\alpha$ -radiation ( $\lambda=1.5406 \text{ \AA}$ ) operated at room temperature. The XRD spectra was recorded in the diffraction angle ( $2\theta$ ) range,  $10$ - $80^\circ$  with a step size of ( $2\theta$ )  $0.0331^\circ$ . The composition of the films was estimated using EDS attached to Field Emission Scanning Electron Microscopy (FESEM, Model: Inspect<sup>TM</sup> S50) operated at an accelerated voltage of 20 kV. The nature of surface morphology was analyzed using both FESEM and atomic force microscopy (AFM, Model: Innova SPM Atomic Force Microscope). The valence (oxidation) state of constituent elements of SnS layers were confirmed using X-ray photoelectron spectroscopy (XPS: Kratos XPS Ultra DLD). The Raman spectroscopy (Lab RAM HR Raman) was operated in backscattering mode using Nd-YAG laser with excitation wavelength 532 nm to identify the phases present in the films. The electrical conductivity of the films was studied by Hall effect technique. The transmittance spectra of the films were recorded using a UV-VIS-NIR Spectrophotometer (Model: Shimadzu UV-3600 UV-VIS-NIR Spectrophotometer) over the wavelength range 300-2000 nm to estimate the energy band gap and absorption coefficient.

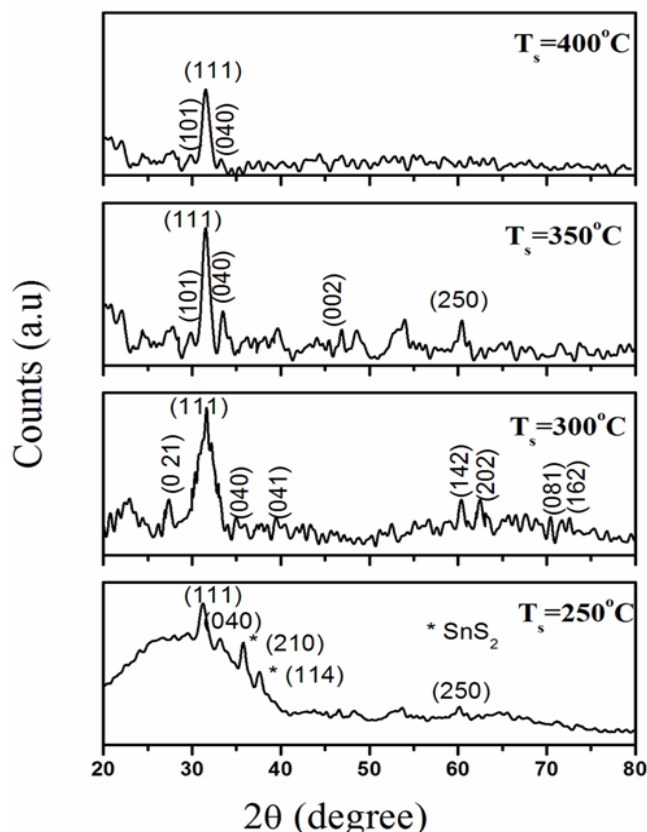


Fig. 1. XRD spectra of Sn layers sulfurized at  $250^\circ\text{C}$ ,  $300^\circ\text{C}$ ,  $350^\circ\text{C}$  and  $400^\circ\text{C}$ .

## Results and discussion

### Structural properties

The visual observation of Sn precursor sulfurized at various temperatures indicates that the films were pin-hole free and uniform. The scotch tape test confirms that the layers were strongly adhered to the substrate surface. **Fig. 1** shows the X-ray diffraction pattern of the Sn layers sulfurized at various temperatures. It is observed that the films sulfurized at  $T_s = 250$  °C, shows (210) and (114) planes of  $\text{SnS}_2$  at  $34.8^\circ$  and  $36.4^\circ$  in addition to various peaks corresponding to SnS phase [29, 30]. With the increase of sulfurization temperature to  $300^\circ\text{C}$ ,  $\text{SnS}_2$  dissociated into SnS and S, resulting in the complete SnS formation and exhibited the (111), (040), (002) and (250) planes that corresponds to the orthorhombic crystal structure of SnS [31, 32]. The further rise in temperature from 300 to  $350$  °C, the intensity of the (111) plane became stronger, which indicates that the layers are completely transformed into orthorhombic SnS with improved crystallinity. Further raise in temperature to  $400$  °C leads to re-evaporation of film due to variation in partial pressures at elevated temperatures.

The crystallite size ( $D$ ) and lattice strain ( $\epsilon$ ) was calculated using XRD data from the following relations.

$$D = \frac{K\lambda}{\beta \cos\theta} \quad (1)$$

$$\epsilon = \frac{\beta \cos\theta}{4} \quad (2)$$

where,  $K$  is constant and is '1' for spherical shape crystallites,  $\lambda$  is the wavelength of the  $\text{CuK}\alpha$  X-rays,  $\beta$  is the full width at half maximum intensity of the (111) plane,  $\theta$  is the Bragg diffraction angle. Table 1 shows the variation of crystallite size and lattice strain with sulfurization temperature. From the **Table 1**, it can be noticed that the crystallite size was increased while the lattice strain was decreased with the sulfurization temperature and reaching their maximum crystallite size, 30 nm and lowest strain,  $28 \times 10^{-4}$  at  $350$  °C.

**Table 1.** Structural parameters of SnS films.

Sulfurization Temperature (°C)	Crystalline size (nm)	Strain ( $\times 10^{-4}$ )
250	14.33	97
300	19.77	64
350	30.01	28
400	29.06	31

### Raman spectroscopy analysis

Further, the structure of the SnS films was studied in detail using Raman spectroscopy, since the Raman vibrational spectrum related directly to the mean bonding states in the coordination poly-hedra of a material. In orthorhombic SnS, 24 vibrational modes are represented by the following irreducible representations at the center of Brillouin zone.

$$T = 4A_g + 2B_{1g} + 4B_{2g} + 2B_{3g} + 2A_u + 4B_{1u} + 2B_{2u} + 4B_{3u}$$

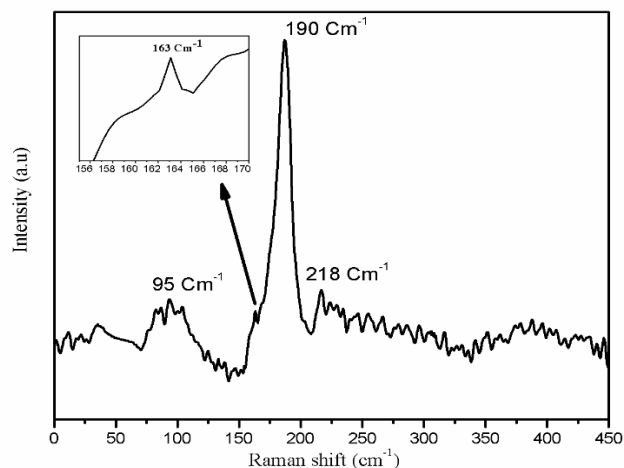


**Fig.2.** Raman spectra of the Sn precursor film sulfurized at  $350$  °C.

Among them, there are 21 optical phonons, of which 12 are Raman active modes ( $4A_g$ ,  $2B_{1g}$ ,  $4B_{2g}$  and  $2B_{3g}$ ), 7 are infrared active modes ( $3B_{1u}$ ,  $1B_{2u}$  and  $3B_{3u}$ ) and 2 are inactive ( $2A_u$ ) [33]. **Fig. 2** shows the Raman spectra of the SnS thin film sulfurized at temperature of  $350$  °C. In the range of  $50$ – $400$   $\text{cm}^{-1}$ , there are three distinct major peaks and one minor peak corresponding to the  $A_g$  mode and  $B_{2g}/B_{3g}$  of SnS were clearly seen at  $95$   $\text{cm}^{-1}$ ,  $190$   $\text{cm}^{-1}$ ,  $218$   $\text{cm}^{-1}$  and  $163$   $\text{cm}^{-1}$  respectively. The observed vibrational modes are in good agreement with the literature and group theory analysis of SnS discussed by Chandrasekhar *et al.* [34] Sohila *et al.* [35]. None of the Raman peaks corresponding to  $\text{SnS}_2$  ( $312$   $\text{cm}^{-1}$ ) and  $\text{Sn}_2\text{S}_3$  ( $307$   $\text{cm}^{-1}$ ) were observed and thus confirming the single-phase growth of SnS.

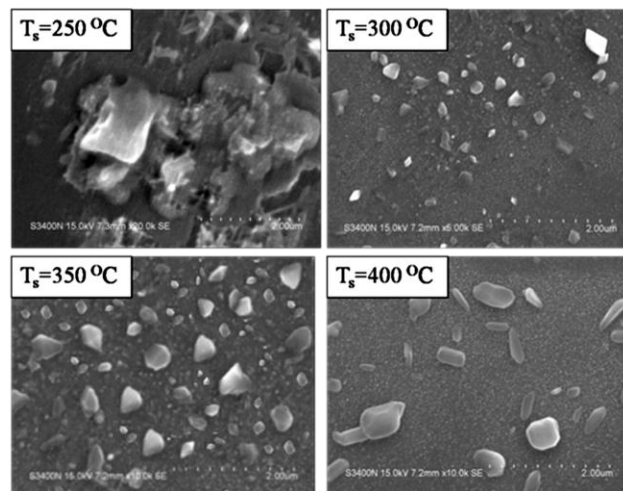


**Fig.3.** SEM images of Sn precursor layers sulfurized at different temperatures.

### Microstructure and composition

The SEM observations demonstrate that the surface morphology of films depends on sulfurization temperature and the corresponding images are shown in **Fig. 3**. The film sulfurized at  $250$  °C had agglomeration appearance while the films sulfurized at  $T_s = 300$  °C consisting more number of smaller spherical grains. The size of these

grains increased with increase of  $T_s = 350\text{ }^\circ\text{C}$  and they are uniform without cracks, but however, the grains are not densely packed. Further increase of  $T_s$  to  $400\text{ }^\circ\text{C}$  had shown smoother morphological features with reduced number of grains, which is due to the partial re- evaporation of sulfur.

The chemical composition of SnS films was evaluated by EDS and found significant changes in the composition of Sn and S with sulfurization temperature. The variation of Sn to S atomic ratio with  $T_s$  is shown in Fig. 4, which indicates the loss of sulfur content in the layers with the increase of  $T_s$ . The films grown at  $T_s = 250\text{ }^\circ\text{C}$  are sulfur rich in nature with Sn/S atomic ratio of 0.69, however, with the increase of sulfurization temperature to  $350\text{ }^\circ\text{C}$ , the Sn/S ratio attained stoichiometry i.e. Sn/S ratio is 1.0 and thereafter a significant loss of Sn has been noticed.

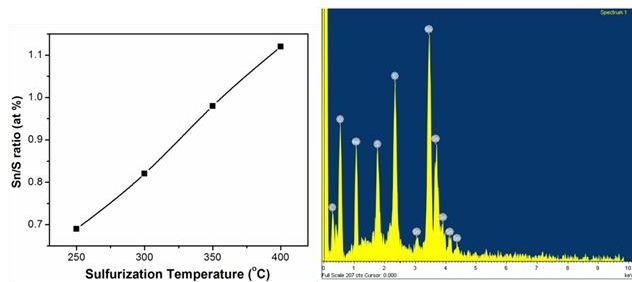


Fig.4. Variation of Sn to S atomic ratio with Sulfurization temperature (left) and EDS spectra of Sn precursors sulfurized at  $350\text{ }^\circ\text{C}$  (right).

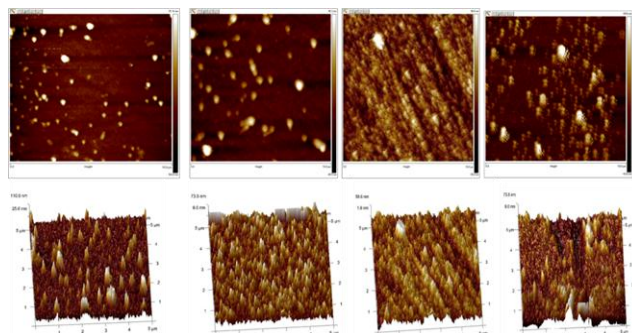


Fig.5. The planar (top) and 3D (bottom) view of AFM pictures of Sn layers sulfurized at temperatures  $250\text{ }^\circ\text{C}$ ,  $300\text{ }^\circ\text{C}$ ,  $350\text{ }^\circ\text{C}$  and  $400\text{ }^\circ\text{C}$ .

**AFM analysis**

The planar and 3D view of AFM images for Sn films sulfurized at different temperatures are shown in Fig. 5. It is observed that the films sulfurized at  $250\text{ }^\circ\text{C}$  revealed that the grains are sparsely distributed on the surface. On the other hand, the morphology of the Sn films sulfurized at  $350\text{ }^\circ\text{C}$  was compact, dense, uniform and smooth since the resulting films are single phase SnS as evidenced from XRD and Raman analysis. The increase in sulfurization temperature leads to the formation of SnS films with good crystalline and uniform distribution of grains. The surface roughness of the films is found to be 10-20 nm.

**Optical properties**

The optical transmittance (T) spectra of the sulfurized Sn precursors were recorded in the wavelength range

300-2000 nm at room temperature using un-polarized light operated at normal incidence. Fig. 6(a) shows the corresponding optical transmittance spectra as a function of wavelength for typical Sn films sulfurized at various temperatures. The T versus  $\lambda$  shows a sudden drop in the transmittance below 850 nm for all the films indicating the onset of absorption for respective phases. The absorption edge shifted from lower wavelength region to higher wavelength with the increase of  $T_s$ . The presence of additional humps in the films sulfurized at  $T_s = 250\text{ }^\circ\text{C}$  can be attributed to the absorption regions corresponding to the SnS<sub>2</sub> and SnS as evidenced by XRD analysis. While the films sulfurized at  $350\text{ }^\circ\text{C}$  shows a perfect steep absorption edge related to SnS. The optical absorption coefficient ' $\alpha$ ' was determined from the transmittance data [ $\alpha = \left(\frac{1}{t}\right) \ln\left(\frac{1}{T}\right)$ ] and found to be  $\sim 5 \times 10^4\text{ cm}^{-1}$ .

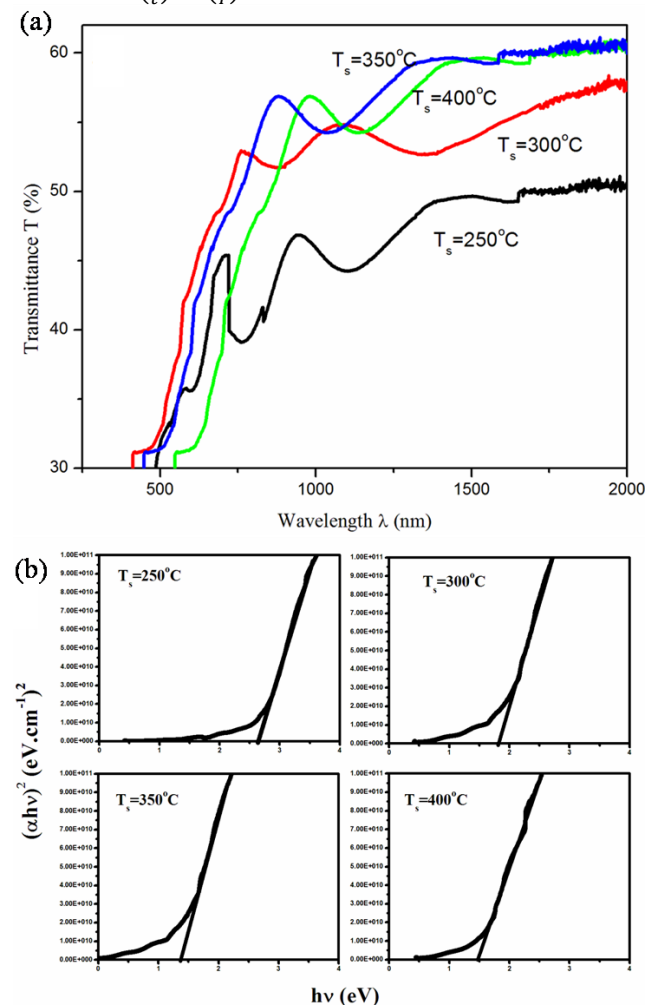


Fig.6. (a) Transmittance Vs. Wavelength spectra and (b)  $(\alpha hv)^2$  Vs. hv plot of Sn layers sulfurized at different temperatures.

The energy band gap of the films was estimated using the following relation.

$$\alpha hv = A(hv - E_g)^n \tag{3}$$

where 't' is thickness of the film ( $\sim 0.5\text{ }\mu\text{m}$ ), A is a constant and 'hv' is incident photon energy. In the present study, Eq. (3) is satisfied for  $n=1/2$  indicating a direct

allowed transition for all the films corresponding to different sulfurization temperatures [36]. The optical band gap of the films was estimated by extrapolating linear part onto 'hv' axis in  $(\alpha hv)^2$  versus hv plots as shown in Fig. 6(b). The films sulfurized at  $T_s = 250$  °C showed an optical band gap close to 2.24 eV. The high energy band gap of the layers might be due to the presence of SnS<sub>2</sub> ( $E_g = 2.44$  eV) [37] as identified by XRD whereas for the films formed at sulfurization temperature,  $T_s = 350$  °C had nearly constant value of energy band gap close to 1.35 eV. It is in good agreement with the reported data for SnS films grown by closed-spaced vapor transport [38].

### XPS analysis

Fig. 7 shows the wide scan core level XPS spectrum of Sn 3d and S 2p for Sn layers sulfurized at 350 °C. The Sn 3d spectrum showed two spin orbit split peaks corresponding to Sn 3d<sub>5/2</sub> and Sn 3d<sub>3/2</sub> located at 485.7 eV and 494.1 eV, respectively. The energy separation between these two peaks is 8.4 eV, which is in agreement with the literature values for Sn in +2 state [39]. The S 2p spectrum of sulfur shows 2p<sub>3/2</sub> and 2p<sub>1/2</sub> peaks located at 161.41 eV and 162.58 eV with a separation of 1.1 eV and is in consistence with the reported range, 160 to 164 eV for S in sulfide form [40].

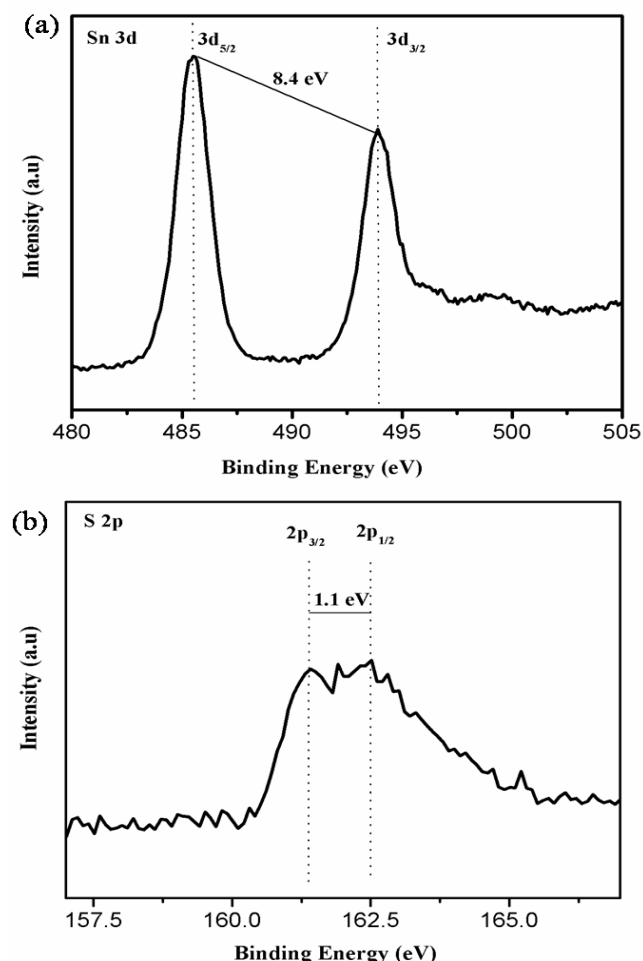


Fig. 7. Typical high-resolution core level XPS spectra of (a) Sn 3d and (b) S 2p for Sn precursor film at 350 °C.

### Electrical analysis

Hot probe test reveals that all the films shown p-type conductivity. The electrical conductivity of the SnS films as a function of sulfurization temperature is shown in Fig. 8. The conductivity was slowly increased from  $2.5 \times 10^{-3}$  ( $\Omega \text{ cm}$ )<sup>-1</sup> to  $1 \times 10^{-2}$  ( $\Omega \text{ cm}$ )<sup>-1</sup> with the increase of  $T_s$  and the Sn layers sulfurized at  $T_s = 350$  °C have shown  $0.947 \times 10^{-2}$  ( $\Omega \text{ cm}$ )<sup>-1</sup>. The low conductivity observed for the layers sulfurized at  $T_s = 250$  °C was to the presence of mixed phases, change in grain size, and also the composition of the films. The high conductivity for the films sulfurized at 400 °C might be due to the decrease in sulfur content as seen in EDS analysis that causes relative increase of tin in the films. The presence of excess tin might create excess of charge carriers in the films, leading to high conductivity for  $T_s = 400$  °C [41].

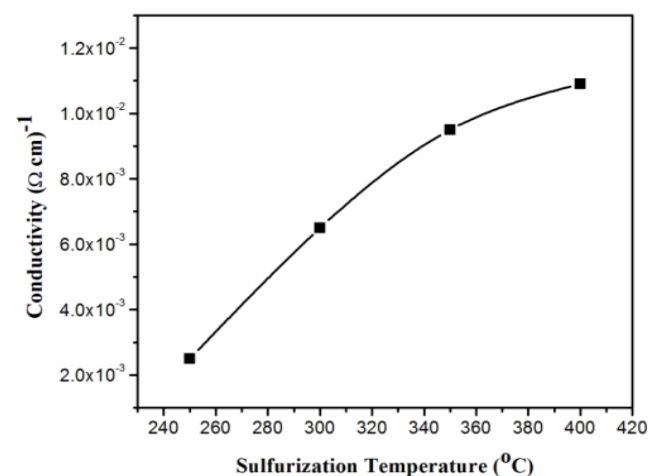


Fig. 8. Variation of Electrical Conductivity of SnS films with respect to Sulfurization temperatures

### Conclusions

In Summary, Tin mono-sulfide (SnS) thin films have been successfully grown using two-step process consisting of sputtered Sn precursors followed by sulfurization. It was found that sulfurization temperature has a great impact on physical properties of SnS thin-films. XRD and Raman study revealed the formation of the high crystalline orthorhombic SnS without any secondary phases at sulfurization temperature,  $T_s = 350$  °C. The crystallite size calculated from (111) plane is found to be 30 nm. XPS analysis confirmed the valence states of Sn<sup>+2</sup> and S<sup>-2</sup> in SnS. The Sn precursors sulfurized at 350 °C have shown optical band gap of 1.35 eV with electrical conductivity  $0.947 \times 10^{-2}$  ( $\Omega \text{ cm}$ )<sup>-1</sup>. The perfect single-phase growth of SnS is an important step towards the realization of high efficiency SnS based solar cells.

### Acknowledgements

Mr. Gurubhaskar is thankful to University Grant Commission (UGC) New Delhi, India for the financial support under RGNFD (F./2013-14/RGNF-2013-14D-OBC-AND-56513). The authors also thank the Department of Science and Technology (DST), Govt. of India for the award of FIST grants (No. SR/FST/PSI-182/2013(C), dated: 25th June 2014).

## References

- Ramakrishna Reddy, K.T.;Forbes, I.; Miles, R.W.; Carter, M.J.;Datta, P.K.; Mater. Lett.,**1998**, 37, 57.  
DOI: [10.1016/S0167-577X\(98\)00066-4](https://doi.org/10.1016/S0167-577X(98)00066-4)
- Miles, R.W.; Ramakrishna Reddy, K.T.; Forbers, I.; J.Crystal Growth,**1999**, 316, 198.  
DOI: [10.1016/S0022-0248\(98\)01036-7](https://doi.org/10.1016/S0022-0248(98)01036-7)
- Kask, E.; Raadik, T.; Grossberg, M.; Josepson, R.;Krustok, J.; Energy Proc.,**2011**, 10, 261.  
DOI:[10.1016/j.egypro.2011.10.188](https://doi.org/10.1016/j.egypro.2011.10.188)
- Adam, W.W.; Baranowski, L.L.; Zawadzki, P.; DeHart, D.; Johnston, S.; Stephan, S.; Wolden, C. A.; Zakutayev, A.; *Prog. Photovolt: Res. Appl.***2016**, 24, 929.  
DOI:[10.1002/pip.2735](https://doi.org/10.1002/pip.2735)
- Koteswara Reddy, N.; Devika, M.; Gopal, E.S.R.; *Critical reviews in solid state and materials science*, **2015**, 0:1-40.  
DOI: [10.1080/10408436.2015.1053601](https://doi.org/10.1080/10408436.2015.1053601)
- Jesse, T.R.D.; walsh, A.; Pooja, M.P.; Laurie, M. P.; Colombara, D.; Saiful Islam, M.; *Phys. Chem. Chem. Phys.*, **2012**,14, 722.  
DOI: [10.1039/c2cp40916j](https://doi.org/10.1039/c2cp40916j)
- Patel, T.H.;, J. Open Surf. Sci., **2012**, 4, 6.  
DOI: [10.2174/1876531901204010006](https://doi.org/10.2174/1876531901204010006)
- Ramakrishna Reddy, K.T.; Koteswara Reddy, N.; Miles, R.W.; *Sol. Energy Mater. Sol. Cells*, **2006**, 90,304.  
DOI:[10.1016/j.solmat.2006.06.012](https://doi.org/10.1016/j.solmat.2006.06.012)
- Ham, G.;Shin, S.;Park, J.;Choi, H.;Kim, J.;Lee, Y.A.;Seo, H.;Jeon, H.; *Appl. Mater. Interfaces*, **2013**, 5, 8889.  
DOI: [10.1021/am401127s](https://doi.org/10.1021/am401127s)
- Parentean, M.; Carbone, C.; *Phys. Rev. B*, **1990**, 41, 5227.  
DOI:[10.1103/PhysRevB.41.5227](https://doi.org/10.1103/PhysRevB.41.5227)
- Nair, M.T.S.; Nair, P.K.; *Semicond. Sci. Technol.*, **1991**, 6, 132.  
DOI: [10.1088/0268-1242/6/2/014](https://doi.org/10.1088/0268-1242/6/2/014)
- Ichimura, M.; Takeuchi, K.; Ono, Y.; Arai, E.; *Thin Solid Films*, **2000**, 361, 98.  
DOI:[10.1016/S0040-6090\(99\)00798-1](https://doi.org/10.1016/S0040-6090(99)00798-1)
- Johnson, J.; Jones, H.; Latham, B.; Parker, J.; Engelken, R.; Barber, C.;*Semicon. Sci. Technol.*, **1999**, 14, 501.  
DOI:[10.1088/0268-1242/14/6/303](https://doi.org/10.1088/0268-1242/14/6/303)
- Ghosh, B.; Bhattacharjee, R.; Banerjee, P.; Das, S.; *Appl. Surf. Sci.*, **2011**, 257, 3670.  
DOI:[10.1016/j.apsusc.2010.11.103](https://doi.org/10.1016/j.apsusc.2010.11.103)
- Caballero, R.; Conde, V.; Leon, M.; *Thin Solid Films*, **2016**, 612, 201.  
DOI:[10.1016/j.tsf.2016.06.018](https://doi.org/10.1016/j.tsf.2016.06.018)
- Parkin, I.P.; Price, L.S.; Hibbert, T.G.;Molloy, K.C.; J. Mater. Chem., **2001**, 11, 1486.  
DOI: [10.1039/B009923F](https://doi.org/10.1039/B009923F)
- Kim, J.Y.; George, S.M.; J. Phys. Chem. C, **2010**, 114, 17597.  
DOI: [10.1021/jp9120244](https://doi.org/10.1021/jp9120244)
- Sinsermsuksakul, P.; Heo, J.; Noh, W.;Hock, A.S.; Gordon, R.G.; *Adv. Energy Mater*, **2011**, 1, 1116.  
DOI: [10.1002/aenm.201100330](https://doi.org/10.1002/aenm.201100330)
- Ortiz, A.; Alonso, J.C.; Goucia, M.; Toriz, J.*Semicond. Sci. Technol.*, **1996**, 11, 243.  
DOI: [10.1088/0268-1242/11/2/017](https://doi.org/10.1088/0268-1242/11/2/017)
- Ramakrishna Reddy, K. T.; Purandhara Reddy, P.; Miles, R.W.; Datta, P.K.; *European Materials Research Society Conf. Strasbourg*, France, **2000**.  
DOI:[10.1016/S0925-3467\(01\)00052-0](https://doi.org/10.1016/S0925-3467(01)00052-0)
- Thangarajan, B.L.; Kaliannan, P.; *J.Phys. D: Appl. Phys*, **2000**, 33, 1054.  
DOI: [10.1088/0022-3727/33/9/304](https://doi.org/10.1088/0022-3727/33/9/304)
- Jayachandran, M.; Mohan, S.; Subramanian, B.; Sanjeeviraja, C.; Ganesan, V.; *J. Mater. Sci. Lett.*,**2000**, 20, 381.  
DOI:[10.1023/A:1006731013279](https://doi.org/10.1023/A:1006731013279)
- Steinmann, V.; Jaramillo, R.; Hartman, K.; Chakraborty, R.; Brandt; R.E.; Poindexte, J. R.; Lee, Y.S.; Sun, L.; Polizzotti ,A.; Park, H.H.; Gordon, R.G.; Buonassisi, T.; *Adv. Mater.*, **2014**, 26, 7488.  
DOI: [10.1002/adma.201402219](https://doi.org/10.1002/adma.201402219)
- Loferski, J.J., *J. Appl. Phys.*,**1956**, 27, 777.  
DOI:[10.1063/1.1722483](https://doi.org/10.1063/1.1722483)
- Chandrasekharan, R., Numerical Modeling of Tin Based Absorber Devices for Cost Effective Solar Photovoltaics, the Graduate School John and Willie Leone Family Department of Energy and Mineral Engineering, The Pennsylvania State University, May 2012.
- Sugiyama, M.; Murata, Y.; Shimizu, T.; Ramya, K.; Venkataiah, C.; Sato, T.; Reddy, K. T. R.;*Jpn. J. Appl. Phys.*, **2011**, 50, 05HF03.  
DOI:[10.1143/JJAP.50.05HF03](https://doi.org/10.1143/JJAP.50.05HF03)
- J Nozik, A.; Coniber, G.; C Beard, M. Advanced Concepts in Photovoltaics; Peater, L.; Frei, H.; Rinaldi, R. (Eds.); The Royal Society of Chemistry: Cambridge UK , 2014, chapter 5 pp.122.  
DOI: [10.1039/9781849739955](https://doi.org/10.1039/9781849739955)
- Vasudeva Reddy, M.R.; Sreedevi, G.; Chinho, P.; Miles, R.W.; Ramakrishna Reddy, K.T.;*Current Applied Physics*,**2015**, 15, 588.  
DOI:[10.1016/j.cap.2015.01.022](https://doi.org/10.1016/j.cap.2015.01.022)
- Lopez, S.; Ortiz, A.; *Semicond. Sci. Technol.*, **1994**, 9, 2130.  
DOI: [10.1088/0268-1242/9/11/016](https://doi.org/10.1088/0268-1242/9/11/016)
- Sanchez-Juarez, A.; Ortiz, A.; *J. Electrochem. Soc.*, **2000**, 147, 3708.  
DOI: [10.1149/1.1393962J](https://doi.org/10.1149/1.1393962J)
- Lefebvre, I.; Lannoo, M.; Olivier-Fourcade, J.; Jumas, J. C.; *Phys. Rev.B*, **1991**, 44, 1004.  
DOI:[10.1103/PhysRevB.44.1004.pdf](https://doi.org/10.1103/PhysRevB.44.1004.pdf)
- JCPDS—Powder Diffraction File 39-354, Swarthmore, PA, **1991**.
- Nikolic, P. M.; Lj Milikovic, P.; Mihajlovic, B.; Lavrencic; J. *Phys. C: Solid State Phys.*, **1977**, 10, L289.  
DOI: [10.1088/0022-3719/10/11/003](https://doi.org/10.1088/0022-3719/10/11/003)
- Chandrasekhar, H.R.; Humphreys, R.G.; Zwick, U.; Cardona, M.; *Phys. Rev. B*, **1977**, 15, 2177.  
DOI: [10.1103/PhysRevB.15.2177](https://doi.org/10.1103/PhysRevB.15.2177)
- Sohila, S.;Rajalakshmi, M.;Ghosh, C.;Arora, A.K.; Muthamizhchelvan, C.; *J. Alloys Compd.*, **2011**, 509, 5843.  
DOI: [10.1016/j.jallcom.2011.02.141](https://doi.org/10.1016/j.jallcom.2011.02.141)
- Kawano, K.; Nakata, R.; Sumita, M.; *Phys. D* **1989**,22, 136.  
DOI: [10.1088/0022-3727/22/1/019](https://doi.org/10.1088/0022-3727/22/1/019)
- Thangaraju, B.; Kaliannan, P.; *J. Phys. D: Appl. Phys.*; **2000**, 33, 1054.  
DOI: [10.1088/0022-3727/33/9/304](https://doi.org/10.1088/0022-3727/33/9/304)
- Yanuar, F.; Guastavino, C.; Llinares, K.; Djessas, G.; Masse, J.; *Mater. Sci. Lett.*, **2000**, 19, 2135.  
DOI:[10.1023/A:1026778810656](https://doi.org/10.1023/A:1026778810656)
- Moulder, J. F.; Stickle, W.F.;Sobol, P.E.;Bomben, K.D.,*Handbook of X-ray Photoelectron Spectroscopy*, Perkin-Elmer Corporation, USA, **1992**.
- Briggs, D.; Peah M. (Eds.), *Practical Surface Analysis*, Wiley, Chichester, **1990**.
- Ristov, M.; Sinadinovski, Gj.; Grozdanov, I.; Mitreski, M.; *Thin Solid Films*, **1989**, 53, 173.  
DOI: [10.1016/0040-6090\(89\)90536-1](https://doi.org/10.1016/0040-6090(89)90536-1)